Research Article

Methodological Approach to Accuracy Assessment in CAD-CAM Mandibular Reconstruction

Elisa Vargiu[1], Giorgia Menapace[2], Giordana Bettini[3], Laura Tognin[2], Sandi Andrea[4], Michelon Fabio[4], Giorgia Saia[5], Giorgio Bedogni[6,7], Meneghello Roberto[1], Alberto Bedogni[5,8]

1. Department of Management and Engineering, University of Padua, Italy; 2. Unit of Maxillo-Facial Surgery, Head and Neck Department, University of Parma, Italy; 3. Maxillofacial Surgery Unit, "S. Anna" Hospital, Italy; 4. Independent researcher; 5. Department of Neuroscience, Unit of Maxillofacial Surgery, University of Padua, Italy; 6. Department of Medical and Surgical Sciences, University of Bologna, Italy; 7. Department of Primary Health Care, Internal Medicine Unit addressed to Frailty and Aging, "S. Maria delle Croci" Hospital, AUSL Romagna, Italy; 8. Regional Center for the Prevention, Diagnosis, and Treatment of Medication and Radiation-related Bone Diseases of the Head and Neck, Hospital Trust of Padova, Italy

Background. Assessing accuracy in CAD-CAM mandibular reconstruction poses significant challenges but is essential for ensuring reliable outcomes. Existing methods are often operator-dependent, lacking repeatability and reproducibility.

Purpose. This study introduces the Global Positioning Layout (GPL) method, an accuracy assessment technique integrated into the reconstruction protocol based on CAD-CAM and additive printing technology. We describe the methodology and process for applying this approach in detail.

Methods. The GPL method was developed at the University of Padova, Italy. Key principles of accuracy assessment were identified and structured as Requirements, Data input, Data reference system, and Data output. The necessary 3D virtual models were defined: planned mandible, reference mandible, patient-specific implant (PSI), postoperative mandible, and postoperative PSI. A unique coordinate system (GPL-RS) was built on the reference mandible. Three Roto-Translational Matrices (RTMs) were applied to measure movements and deviations between the designed and postoperative models to assess reconstruction accuracy.

Results. A case study of mandibular reconstruction with a CAD-CAM titanium PSI is presented to showcase the GPL methodology. Geomagic Wrap® software is used, utilizing its Python programming tools and GEO and API libraries.

 doi.org/10.32388/CDHISR.2

Conclusion. The GPL method represents a significant advancement in assessing the accuracy of CAD-CAM reconstructions, providing valuable insights that can improve surgical outcomes.

Roberto Meneghello and Alberto Bedogni equally contributed to this work.

Corresponding author: Alberto Bedogni, alberto.bedogni@unipd.it

Introduction

Computer-aided design and manufacturing (CAD-CAM) is an emerging technology in head and neck reconstructive surgery, providing patient-specific devices to restore facial symmetry and volumes [1]. The introduction of additive manufacturing and 3D printing has revolutionized the planning of resections and reconstructions in complex cases [2][3]. Virtual surgical planning (VSP) offers a 3D visualization of patient anatomy for personalized surgical planning [4]. Computer-assisted surgery (CAS) enhances precision and reduces the surgeon's learning curve [5]. CAD-CAM technology also provides objective data to ensure consistency. However, VSP may increase patient expectations before surgery [6]. Despite these advancements, evaluating the accuracy of CAD-CAM mandibular reconstruction is challenging, with no standardized protocols for VSP, virtual design, or additive printing in customized reconstructive surgery [7]. To optimize outcomes, CAS performance should be quantitatively assessed [8][9]. Several methods have been developed to assess CAD-CAM mandibular reconstruction accuracy, including comparisons of 2D CT images and 3D CT scans[10]. Some methods rely on linear and angular measures based on the distance between anatomical landmarks. Such landmarks are drawn as single points on two-dimensional CT images or 3D virtual model surfaces [11][12][13][14][15][16][17]. These methods, however, are operator-dependent and may lack repeatability. A guideline has been recently proposed to standardize evaluation methods, including strategies for imaging, defect classification, data comparison, and volume assessment of 3D models[18]. The Global Positioning Layout (GPL) method was initially developed to quantify the 3D spatial deviation between planned and postoperative reconstructions using roto-translational matrices (RTM) (Menapace G, et al. Personal communication at the 28th National Congress of the Italian Society of Microsurgery, November 21-23, 2019; Genoa, Italy; Bettini G, et al. Personal communication at the 25th Congress of the European Association for Maxillofacial Surgery - EACMFS; July 14-16, 2021; Paris, France). Initially operator-dependent, it has since been refined to eliminate variability.

 doi.org/10.32388/CDHISR.2

This study aims to establish metrological principles for computer-aided accuracy assessment in CAD-CAM mandibular reconstruction and to introduce the GPL method, designed to ensure reliable outcomes independent of software and operator.

Methods

Study setting

The GPL method was developed at the Departments of Neuroscience-DNS and of Management and Engineering of the University of Padova (Italy). This study was conducted in full accordance with the principles outlined in the Declaration of Helsinki.

Basic principles of accuracy assessment

The basic principles of accuracy assessment are listed as follows:

A. Requirements:
   a. Functionality: computing of spatial relationships between the planned mandibular reconstruction and the postoperative result.
   b. Independency: results shall be independent of the operator (Operator uncertainty principle), thus minimizing human error and variability in measurements.
   c. Compatibility: input and output data shall be given in a format suitable for any CAD-based system.
   d. Generality: the methodology should apply to various mandibular defects and reconstruction procedures, allowing for broad clinical use.
   e. Rigid workpiece: any patient-specific device is a rigid part of infinite stiffness or whose distortion does not exceed specified tolerances by applying pressure or forces during and after standard surgery. It provides a stable reference for accuracy assessment.

B. Data input:
   1. any kind of mandibular bone defect.
   2. any kind of VSP of mandible reconstruction.
   3. any kind of CAD patient-specific device.

C. Data reference system:

1. a defined and unique, intrinsic, 3D coordinate system (X-Y-Z), called "reference system", is used to describe the spatial position and orientation of any model.

D. Data output:

1. a three-dimensional assessment of spatial errors, according to the reference system
2. errors concern the position and orientation of the patient-specific device.

Definition of operational models for GPL applications

The Digital Imaging and Communications in Medicine (DICOM) data obtained from the preoperative CT scans are imported into a given virtual planning software and converted into surface models in a Standard Tessellation Language (STL) file format.

The virtual 3D model (i.e. CAD model) of the facial skeleton is segmented to obtain the "*native mandible*", which consists of the entire mandible, including both the diseased and healthy parts. The native mandible is used to extract the "*planned mandible*", which consists of the healthy portion of the native mandible devoid of the diseased bone.

For bone defects limited to half of the mandible, the native mandible is mirrored and fitted to obtain the *"reference mandible"*. In case of gross deformation of the mandible exceeding the midline, the reference mandible is obtained through superimposition, scaling, and fitting of healthy 3D models of the mandible taken from a virtual image library of lower jaws.

Then, the reference mandible is used to design the patient-specific implant (PSI). The final virtual 3D model of the device is called "*designed PSI*". The combination of the planned mandible and the designed PSI is called the "*designed model*".

The virtual 3D model of the postoperative result is obtained from the postoperative CT scans using the same approach and is called the "*postoperative model*". This latter consists of the combination of two features: *the "postoperative mandible"*, which is the remaining portion after surgical resection of the diseased bone volume, and *the "postoperative PSI"*, which is the patient-specific implant following surgical implantation. The sequence of the operational models is depicted in Figure 1:

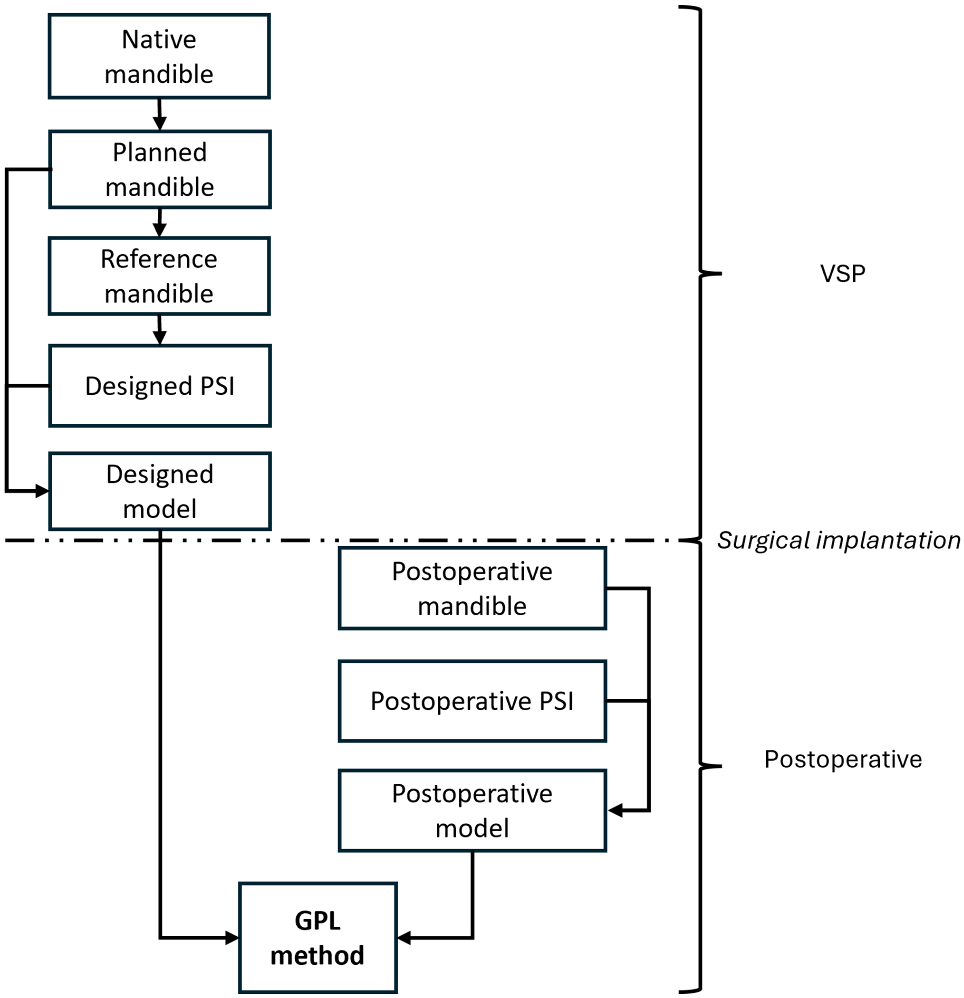

Figure 1. *Sequence of models obtained from the Virtual Surgical Planning and the Postoperative follow-up.*

In conclusion, the following virtual 3D models are required to apply the GPL method: planned mandible, reference mandible, designed PSI, postoperative mandible, and postoperative PSI.

GPL data coordinate reference system

In the GPL method, the virtual 3D models of the VSP are positioned and aligned in a unique coordinate (X-Y-Z) reference system (GPL-RS). GPL-RS is based on the reference mandible through an automated process of identification of specific geometric features (see § Step 2: Reference system (GPL-RS) definition).

The virtual 3D postoperative model is positioned and oriented in a coordinate reference system that originates from CT data acquisition. Therefore, alignment of the virtual 3D postoperative model to GPL-RS is essential to perform the analysis and comparison according to the GPL methodology.

GPL workflow

The GPL workflow is depicted in Figure 2:

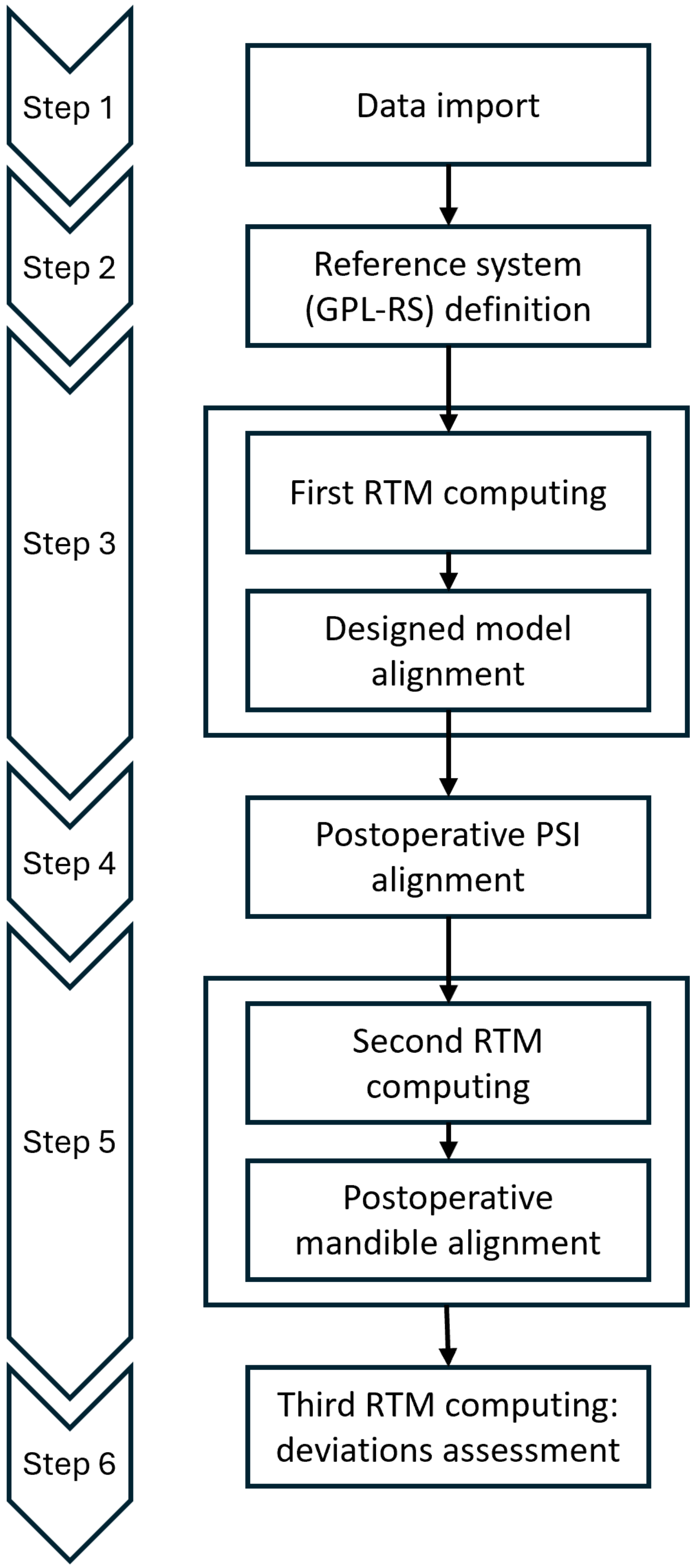

doi.org/10.32388/CDHISR.2

Figure 2. *Global Positioning Layout workflow.*

In the following, a brief description of the main steps is presented:

Step 1: Data import

Five 3D virtual models are imported into the application software: a) planned mandible, b) reference mandible, c) designed PSI, d) postoperative mandible, and e) postoperative PSI.

Step 2: Reference system (GPL-RS) definition

The GPL-RS is constructed on the reference mandible.

In brief, 3 intra-mandibular geometric features are computed: the *centre of gravity (i.e. barycentric point)*, a *symmetry plane,* and a *plane tangent to the inferior edge of the mandible.*

The application software computes the centre of gravity.

The symmetry plane of the reference mandible intentionally passes through the centre of gravity.

The tangent plane to the inferior edge of the mandible is set through an optimization algorithm, which minimizes the distance from the centre of gravity.

To define the GPL-RS, the intra-mandibular geometric features are then associated with the common coordinate reference system (i.e. cartesian coordinate system, XYZ) following the ordered sequence:

1. centre of gravity → OO origin of axes
2. symmetry plane → YZ plane
3. tangent plane to inferior mandibular edge → XY plane

This sequence aligns (i.e. translates and rotates) the *reference mandible* onto the GPL-RS coordinate system.

Step 3: First roto-translational matrix (RTM) computing and designed model alignment

The quantitative estimation of the above-mentioned movements of the reference mandible is described by 3 rotational and 3 translational components according to the X, Y, and Z axes of the GPL-RS, which define the 1st RTM: positive rotation angles cause a counterclockwise rotation around the axes while positive translations cause a movement along the axes.

 doi.org/10.32388/CDHISR.2

Below is provided the general form of the roto-translational matrix:

$$\mathrm{RTM} = \begin{bmatrix} r_{11} & r_{12} & r_{13} & t_x \\ r_{21} & r_{22} & r_{23} & t_y \\ r_{31} & r_{32} & r_{33} & t_z \\ 0 & 0 & 0 & 1 \end{bmatrix} \tag{1}$$

It's a 4x4 matrix where the upper-left 3x3 sub-matrix represents the rotation matrix, and the last column (3x1) of the matrix represents the translational vector.

The 1st RTM is then applied to align *the designed model* (*planned mandible + designed PSI)* to the GPL-*RS*.

Step 4: Postoperative PSI alignment

The *postoperative PSI* is then aligned to the *designed PSI* through two consecutive steps using ICP algorithms. The initial step involves the superimposition of the prosthetic model onto the design model. This is achieved using a best-fit method that minimizes the distance between the two models by automatically selecting corresponding points. In the second step, a more detailed ICP-based alignment is employed to improve the preliminary superimposition.

Step 5: Second roto-translational matrix (RTM) computing and postoperative mandible alignment

The quantitative estimation of the *postoperative PSI* movements is the 2nd RTM. The 2nd RTM is then applied to align the *postoperative mandible* to the *GPL-RS*.

Step 6: Third roto-translational matrix (RTM) computing: measure of deviations

For the assessment of the accuracy in CAD-CAM mandibular reconstruction, the computation of the deviation between the postoperative model and the designed model requires the superimposition of the postoperative mandible onto the designed mandible.

Similarly to the procedure conducted for prosthetic models, it is necessary to undergo two alignment phases.

The quantitative estimation of the *postoperative mandible* movements is the 3rd RTM.

The 3rd RTM represents the deviations (rotational and translational errors) and measures the accuracy of the reconstruction. The general form of the roto-translational matrix is given by equation (1).

The rotational movements along the X, Y, and Z axes performed by the mandible in the postoperative follow-up can be computed employing Euler's formulas:

$$\theta_x = \operatorname{a}\tan 2\left(-r_{23}, r_{33}\right) \tag{2}$$

$$\theta_y = \operatorname{a}\sin(r_{13}) \tag{3}$$

$$\theta_z = \operatorname{a}\tan 2\left(-r_{12}, r_{11}\right) \tag{4}$$

The translations, instead, can be directly extracted from the roto-translational matrix.

$$\mathrm{T} = \begin{bmatrix} tx \\ ty \\ tz \end{bmatrix} \tag{5}$$

Results

The case study of a patient who underwent mandibular reconstruction of a condylar-containing lateral defect with a CAD-CAM titanium patient-specific device at the Unit of Maxillofacial Surgery of the University Hospital of Padua (Italy) is used to showcase the GPL methodology.

Data imaging (DICOM) is obtained from the preoperative and 1-month postoperative CT scans of the selected patient. A detailed description of the VSP and computer-aided mandibular design and fabrication developed at the Unit of Maxillofacial Surgery of the University of Padua (Italy) in collaboration with CAD-CAM specialists (Sintac s.r.l, Biomedical Engineering, Trento, Italy, and 3D-Fast s.r.l, Padova, Italy) has been previously published [19].

On purpose, Geomagic Wrap ® (Oqton Inc., South Carolina, US) is used to present the procedure, taking advantage of its built-in Python programming tool and associated GEO and API libraries. All steps previously described are reproduced with the software, including the roto-translational matrices results for the selected patient.

First, the five 3D virtual models depicted in Figure 3 (planned mandible, reference mandible, designed prosthesis, postoperative prosthesis, and postoperative mandible) are imported into the application software.

doi.org/10.32388/CDHISR.2

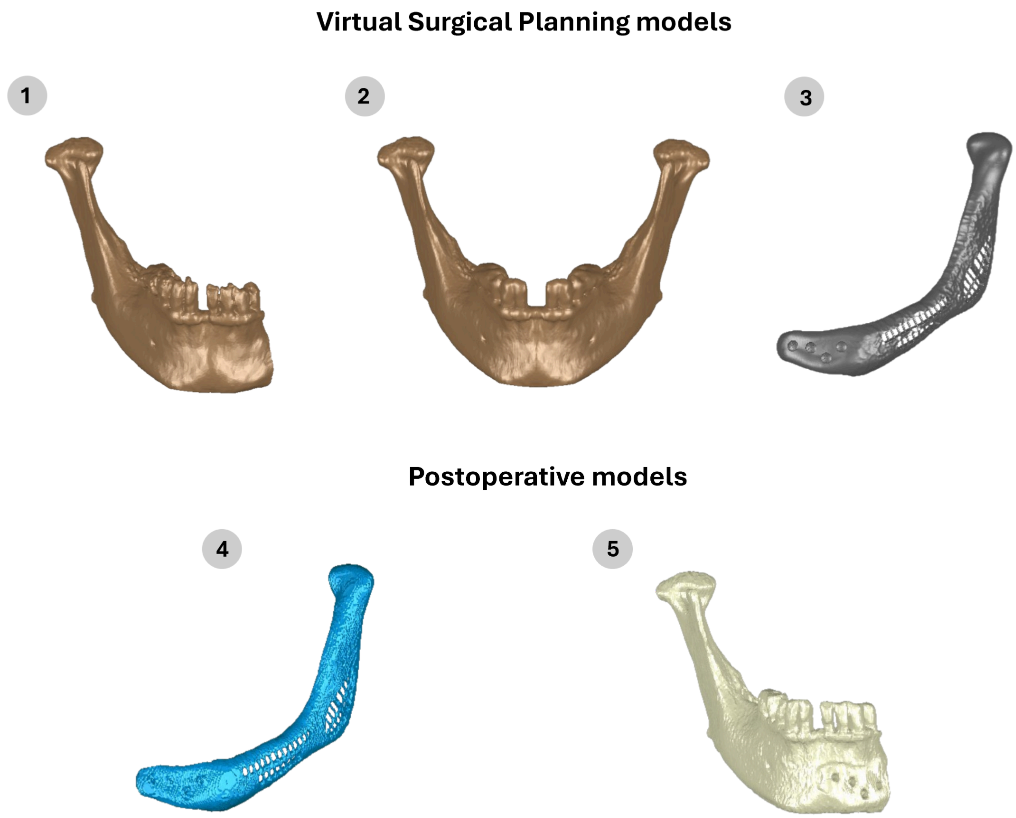

Figure 3. *Five 3D models imported in Geomagic Wrap to apply the GPL method: 1) planned mandible 2) reference mandible 3) design prosthesis 4) postoperative prosthesis 5) postoperative mandible.*

The reference system (GPL-RS) definition and 1st roto-translational matrix (RTM) computing are shown in Figure 4.

doi.org/10.32388/CDHISR.2

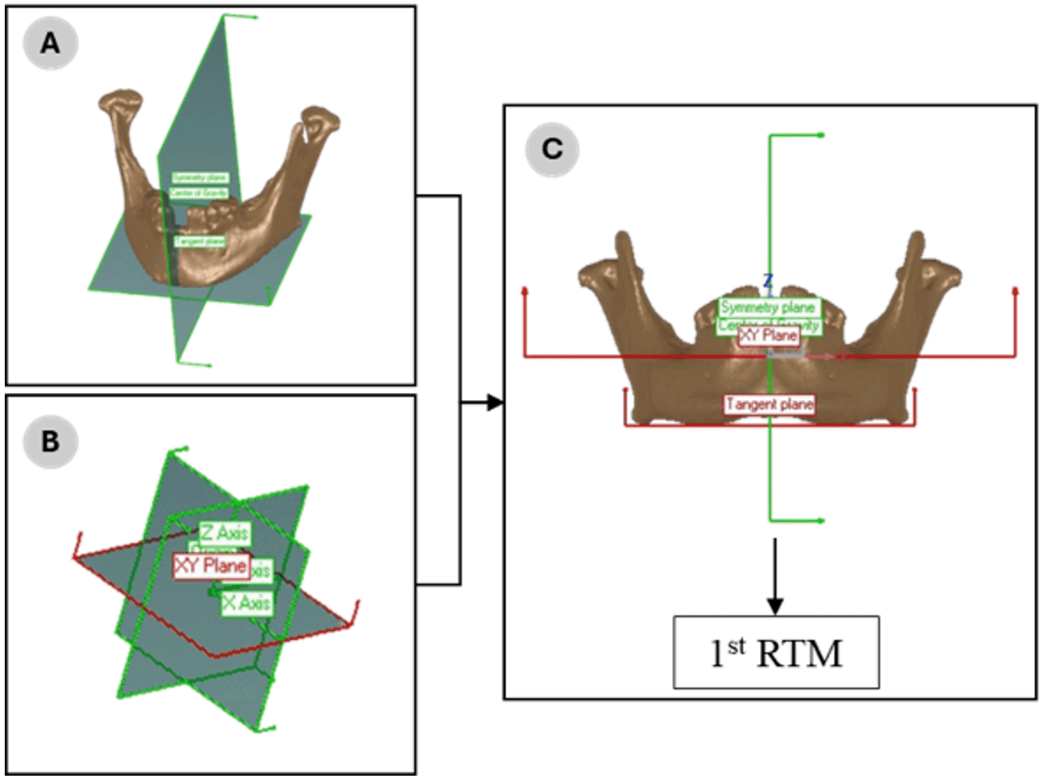

Figure 4. *Reference system (GPL-RS) definition and first RTM computing. 4A: Intra-mandibular geometric features. 4B: World reference system. 4C: Reference mandible aligned to the global reference system.*

In detail, the intra-mandibular geometric features (centre of gravity, symmetry plane, and tangent plane) are used to align the reference mandible to the reference system called *'World'* in Geomagic; thus, the 1st RTM is obtained. The rotations and translations extracted from the 1st RTM are reported in Table 1.

The 1st RTM is applied for the alignment of the designed model (Figure 5A).

In this way, all VSP models are located on the same reference system (Figure 5B). Next, the postoperative prosthesis is aligned to the designed prosthesis through '*Best Fit Alignment*' and *'Global Registration*' commands (Figure 5C); then the 2nd RTM is obtained (Table 1).

doi.org/10.32388/CDHISR.2

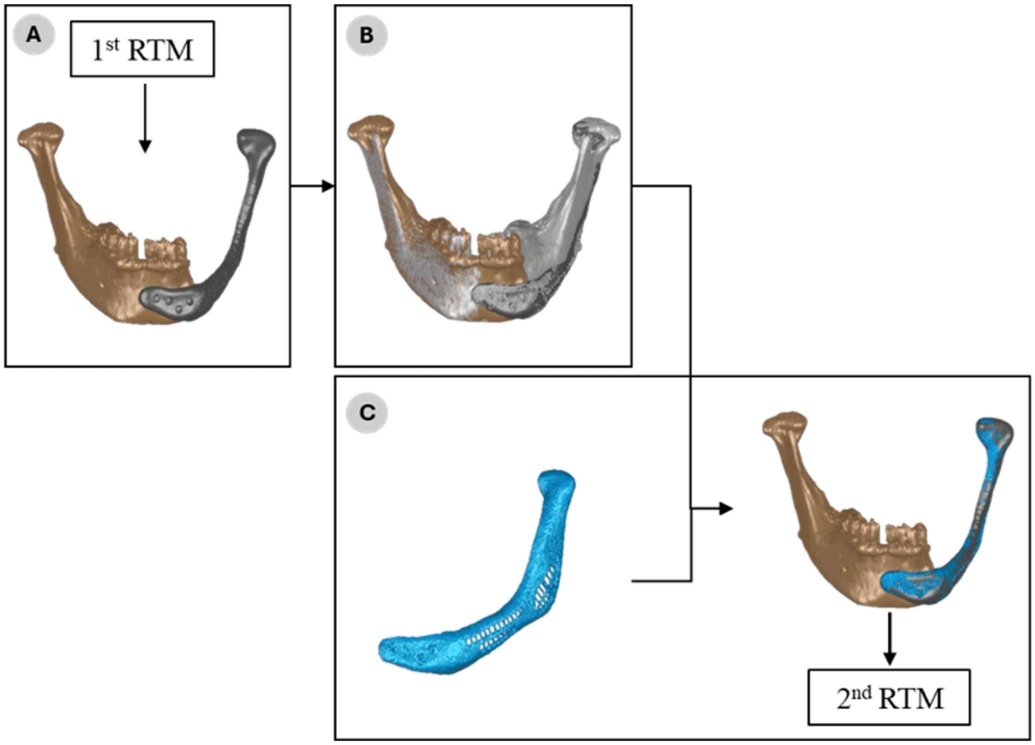

Figure 5. *Alignment of the designed model (5A, 5B), superimposition of the postoperative prosthesis onto the designed prosthesis, and 2nd RTM computing (5C). 5A: Alignment of the designed model. 5B: VSP models in the same reference system. 5C: Alignment of the postoperative prosthesis.*

The 2nd RTM is applied for the alignment of the postoperative mandible (Figure 6A). In this way, all 3D models are located on the same reference system (Figure 6B).

Once aligned with the GPL-RS, the model must be reoriented using the *'reorient model'* function to reset the previously applied movement. Then, the postoperative mandible is aligned to the designed mandible through 'Best Fit Alignment' and 'Global Registration' commands (Figure 6C).

doi.org/10.32388/CDHISR.2

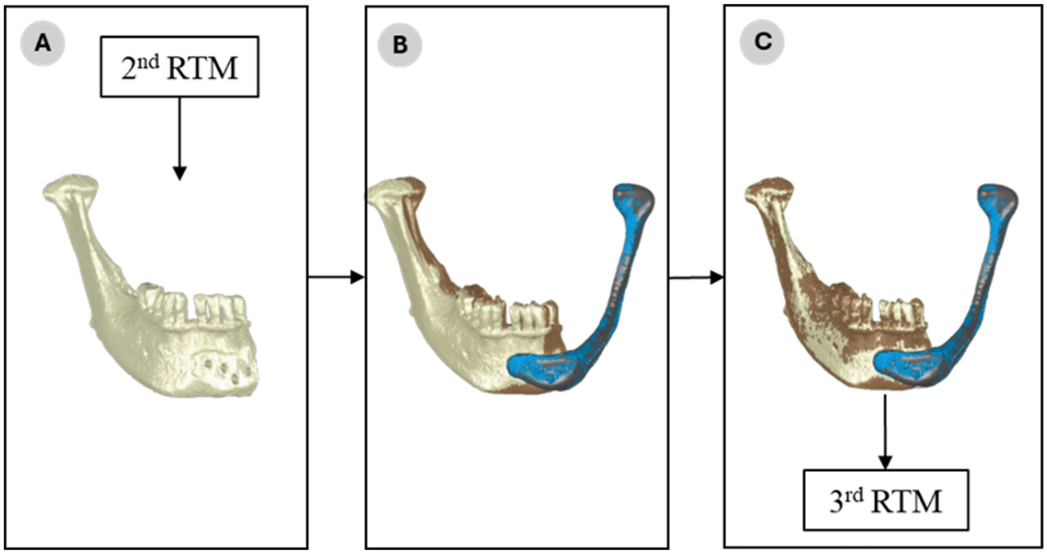

Figure 6. *Postoperative mandible alignment (6A, 6B) and 3rd RTM computing (6C). 6A: Alignment of the postoperative mandible. 6B: All 3D models in the same reference system. 6C: Alignment of the postoperative mandible to the designed mandible.*

Finally, the 3rd RTM is obtained to assess the deviations between the designed model and the post-operative model, which quantifies the accuracy of mandibular reconstruction (Table 1).

	Rot X	Rot Y	Rot Z	Trans X	Trans Y	Trans Z
	[deg]			*[mm]*		
1rt RTM	-19,440	0,026	0,009	4,589	210,497	507,899
2nd RTM	-17,553	-1,272	6,614	-33,448	264,291	136,173
3rd RTM	-3,115	2,112	-2,477	2,213	0,719	-1,922

Table 1. *Rotations and translations obtained from the three roto-translational matrices. The 3rd RTM quantifies the distortion of the mandibular reconstruction.*

To visualize the displacement of the prosthetic implant during the mandibular reconstruction process, it

doi.org/10.32388/CDHISR.2

is necessary to apply the 3rd RTM to the postoperative prosthesis (Figure 7).

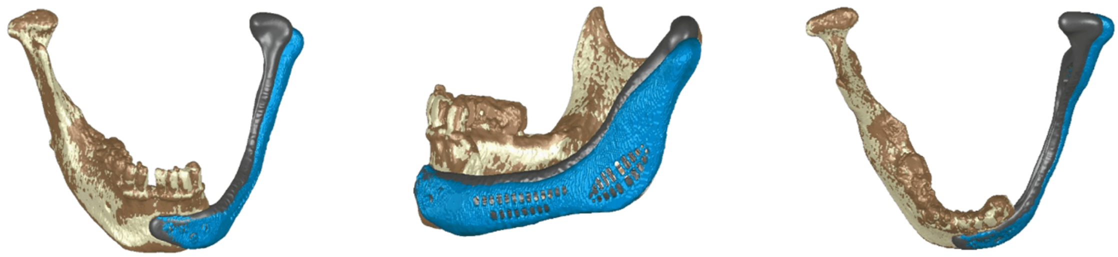

Figure 7. *Application of the 3rd roto-translational matrix to the postoperative prosthesis.*

Discussion

Recently developed computer-assisted reconstructive surgery techniques integrate advanced 3D imaging, computer simulation software, and CAD/CAM technologies [2]. These systems aim to enhance surgical outcomes and ensure reproducibility. The process of computer-assisted surgery (CAS) consists of sequential phases: 1) image data acquisition and elaboration/segmentation, 2) virtual surgical planning (CAD), 3) manufacturing of the final construct (CAM), 4) surgical treatment, and 5) evaluation of the result. Each phase is prone to errors that may impact both the outcome and patients' quality of life [8]. This study introduces the Global Positioning Layout (GPL) method, which compares distortions between the postoperative and planned virtual models. Unlike using the native mandible as a reference, the GPL relies to the planned model, avoiding alterations due to underlying pathological conditions. This approach aligns with the views of other authors [8][11][20][21].

A key feature of GPL is its assumption that the titanium device used in the reconstruction maintains its geometry post-implantation. By first superimposing the titanium device, the method provides a consistent basis for accuracy assessment over time. For this reason, we chose to present the GPL method using a case of mandibular reconstruction with a CAD-CAM titanium patient-specific implant.

While some methods discourage superimposing pre- and postoperative STL models due to reconstruction hardware scattering [8][22][23], GPL minimizes this issue using an ICP algorithm with *Auto-deviation Elimination*, which excludes erroneous points.

Current methods, including GPL, are limited by image data quality. Preoperative and postoperative CT scans may vary due to different scanners and parameters [8].

The GPL method, however, focuses on accuracy assessment, not image acquisition improvements, which remain an active research area [24][25][26].

Van Baar et al. 2019 suggested starting the alignment from the condylar processes of the mandible on the postoperative STL model [18]. However, the condylar unit is often included in the resection plan, limiting its use for superimposition across the full spectrum of mandibular bone defect reconstructions [19][27][28]. Moreover, the condyle can undergo displacement due to mechanical overload, loss of dental elements, detachment/resection of masticatory muscles, or postoperative factors, such as soft-tissue edema [29][30][31][32]. These factors may resolve over time, altering the postoperative anatomy, which complicates long-term accuracy assessment. Current accuracy methods compare early postoperative result (within 1-month post-surgery) to the planned reconstruction [7], but long-term stability of the reconstruction and the impact of clinical factors on the outcome require further analysis. For this reason, the method should be automated and operator-independent and meet all the requirements outlined in the GPL.

Comparing the postoperative and preoperative/planned 3D models usually involves manual selection of anatomical landmarks, which can introduce variability and affect accuracy, especially in the alignment of condylar processes [33]. Manual alignment may lead to inconsistencies, and the final ICP alignment may not always reflect the true anatomical position, complicating clinical decision-making.

Some methods use 3D colorimetric maps to visualize distortions between the planned and postoperative models [17][23][33][34][35], but a clear quantitative measure of deviation is missing.

GPL overcomes the limitation of current methods by using roto-translational matrices to quantify 3D spatial deviations, and by employing a unique reference system (GPL-RS) to describe the spatial position and orientation of any model for any patient. This approach relies on the physical-geometric elements of the reference mandible, which are unique and identifiable for each patient, independent of the severity of any mandibular defect. This ensures consistent and reliable measurements, regardless of operator or software variability.

Bevini et al. (2023) [36] proposed using roto-translational matrices to assess mandibular reconstruction accuracy in 3D. However, their method lacks a standardized reference system, relies on the software's coordinate system, and involves manual PSI superimposition, all which limit reproducibility and increase measurement uncertainty.

Conclusions

The GPL method represents a significant advancement in precision assessment for CAD-CAM mandibular reconstructions, offering valuable insights that can improve surgical outcomes and set new standards in the field of mandibular reconstruction.

Future directions

GPL requires testing and validation across a large cohort of patients, including all types of mandibular defects and CAD-CAM mandibular reconstruction procedures.

Additionally, the GPL workflow requires full automation of the entire process, which will offer significant advantages such as reduced processing times, speeding up accuracy evaluation, and enabling comparisons across large groups. Despite the comprehensive description provided by the matrix components, visualizing the computed deviations between the planned and postoperative mandible remains challenging to translate into a clinical context. Accurate clinical interpretation is crucial, as it allows surgeons to identify errors in reconstructive procedures and implement corrective measures, potentially preventing future mistakes. Enhancing the clinical interpretation of the resulting matrices is an essential task that must be addressed in the future.

References

1. ^*E.I. Chang, M.P. Jenkins, S.A. Patel, N.S. Topham, Long-Term Operative Outcomes of Preoperative Computed Tomography–Guided Virtual Surgical Planning for Osteocutaneous Free Flap Mandible Reconstruction, Plast Reconstr Surg 137 (2016) 619–623. https://doi.org/10.1097/01.prs.0000475796.61855.a7.*
2. a, b*R.D. Largo, P.B. Garvey, Updates in Head and Neck Reconstruction, Plast Reconstr Surg 141 (2018) 271e–285e. https://doi.org/10.1097/PRS.0000000000004070.*
3. ^*N.S.J. Tang, I. Ahmadi, A. Ramakrishnan, Virtual surgical planning in fibula free flap head and neck reconstruction: A systematic review and meta-analysis, Journal of Plastic, Reconstructive & Aesthetic Surgery 72 (2019) 1465–1477. https://doi.org/10.1016/j.bjps.2019.06.013.*
4. ^*R. Pucci, A. Weyh, C. Smotherman, V. Valentini, A. Bunnell, R. Fernandes, Accuracy of virtual planned surgery versus conventional free-hand surgery for reconstruction of the mandible with osteocutaneous free flaps, Int J Oral Maxillofac Surg 49 (2020) 1153–1161. https://doi.org/10.1016/j.ijom.2020.02.018.*

5. ^K.L. Tran, M.L. Mong, J.S. Durham, E. Prisman, Benefits of Patient-Specific Reconstruction Plates in Mandibular Reconstruction Surgical Simulation and Resident Education, J Clin Med 11 (2022) 5306. https://doi.org/10.3390/jcm11185306.
6. ^M. Davey, N.M. McInerney, T. Barry, A. Hussey, S. Potter, Virtual Surgical Planning Computer-aided Design-guided Osteocutaneous Fibular Free Flap for Craniofacial Reconstruction: A Novel Surgical Approach, Cureus (2019). https://doi.org/10.7759/cureus.6256.
7. a, bM.L. Barr, C.S. Haveles, K.S. Rezzadeh, I.T. Nolan, R. Castro, J.C. Lee, D. Steinbacher, M.J. Pfaff, Virtual Surgical Planning for Mandibular Reconstruction With the Fibula Free Flap, Ann Plast Surg 84 (2020) 117–122. https://doi.org/10.1097/SAP.0000000000002006.
8. a, b, c, d, eG.J.C. van Baar, T. Forouzanfar, N.P.T.J. Liberton, H.A.H. Winters, F.K.J. Leusink, Accuracy of computer-assisted surgery in mandibular reconstruction: A systematic review, Oral Oncol 84 (2018) 52–60. https://doi.org/10.1016/j.oraloncology.2018.07.004.
9. ^M.C. Betancourt, C. Araújo, S. Marín, W. Buriticá, The Quantitative Impact of Using 3D Printed Anatomical Models for Surgical Planning Optimization: Literature Review, 3D Print Addit Manuf 10 (2023) 1130–1139. https://doi.org/10.1089/3dp.2021.0188.
10. ^F. Peters, S. Raith, A. Bock, K. Kniha, M. Ooms, S.C. Möhlhenrich, F. Hölzle, A. Modabber, Accuracy of the surgical execution of virtually planned deep circumflex iliac artery flaps and their appropriateness for masticatory rehabilitation, Head Face Med 20 (2024) 42. https://doi.org/10.1186/s13005-024-00444-y.
11. a, bF. Mascha, K. Winter, S. Pietzka, M. Heufelder, A. Schramm, F. Wilde, Accuracy of computer-assisted mandibular reconstructions using patient-specific implants in combination with CAD/CAM fabricated transfer keys, Journal of Cranio-Maxillofacial Surgery 45 (2017) 1884–1897. https://doi.org/10.1016/j.jcms.2017.08.028.
12. ^Y. El-Mahallawy, H.H. Abdelrahman, H. Al-Mahalawy, Accuracy of virtual surgical planning in mandibular reconstruction: application of a standard and reliable postoperative evaluation methodology, BMC Oral Health 23 (2023) 119. https://doi.org/10.1186/s12903-023-02811-8.
13. ^D.J. Annino, R.K. Sethi, E.E. Hansen, S. Horne, T. Dey, E.M. Rettig, R. Uppaluri, J.I. Kass, L.A. Goguen, Virtual planning and 3D -printed guides for mandibular reconstruction: Factors impacting accuracy, Laryngoscope Investig Otolaryngol 7 (2022) 1798–1807. https://doi.org/10.1002/lio2.830.
14. ^F. Wilde, H. Hanken, F. Probst, A. Schramm, M. Heiland, C.-P. Cornelius, Multicenter study on the use of patient-specific CAD/CAM reconstruction plates for mandibular reconstruction, Int J Comput Assist Radiol Surg 10 (2015) 2035–2051. https://doi.org/10.1007/s11548-015-1193-2.

15. ^ *P. Metzler, E.J. Geiger, A. Alcon, X. Ma, D.M. Steinbacher, Three-Dimensional Virtual Surgery Accuracy for Free Fibula Mandibular Reconstruction: Planned Versus Actual Results, Journal of Oral and Maxillofacial Surgery 72 (2014) 2601–2612. https://doi.org/10.1016/j.joms.2014.07.024.*
16. ^ *F. Goormans, Y. Sun, M. Bila, J. Schoenaers, J. Geusens, H.-T. Lübbers, W. Coucke, C. Politis, Accuracy of computer-assisted mandibular reconstructions with free fibula flap: Results of a single-center series, Oral Oncol 97 (2019) 69–75. https://doi.org/10.1016/j.oraloncology.2019.07.022.*
17. a, b *D.M. Chernohorskyi, Y. V. Chepurnyi, O.S. Vasiliev, M. V. Voller, A. V. Kopchak, Evaluation of the accuracy of surgical reconstruction of mandibular defects when using navigation templates and patient-specific titanium implants, Journal of Education, Health and Sport 11 (2021) 117–132. https://doi.org/10.12775/JEHS.2021.11.02.013.*
18. a, b *G.J.C. van Baar, N.P.T.J. Liberton, T. Forouzanfar, H.A.H. Winters, F.K.J. Leusink, Accuracy of computer-assisted surgery in mandibular reconstruction: A postoperative evaluation guideline, Oral Oncol 88 (2019) 1–8. https://doi.org/10.1016/j.oraloncology.2018.11.013.*
19. a, b *A. Bedogni, G. Bettini, G. Bedogni, G. Menapace, A. Sandi, F. Michelon, R. Di Carlo, P. Franco, G. Saia, Safety of boneless reconstruction of the mandible with a CAD/CAM designed titanium device: The replica cohort study, Oral Oncol 112 (2021) 105073. https://doi.org/10.1016/j.oraloncology.2020.105073.*
20. ^ *L. Zhang, Z. Liu, B. Li, H. Yu, S.G. Shen, X. Wang, Evaluation of computer-assisted mandibular reconstruction with vascularized fibular flap compared to conventional surgery, Oral Surg Oral Med Oral Pathol Oral Radiol 121 (2016) 139–148. https://doi.org/10.1016/j.oooo.2015.10.005.*
21. ^ *A. Tarsitano, S. Battaglia, F. Ricotta, B. Bortolani, L. Cercenelli, E. Marcelli, R. Cipriani, C. Marchetti, Accuracy of CAD/CAM mandibular reconstruction: A three-dimensional, fully virtual outcome evaluation method, Journal of Cranio-Maxillofacial Surgery 46 (2018) 1121–1125. https://doi.org/10.1016/j.jcms.2018.05.010.*
22. ^ *R.H. Schepers, J. Kraeima, A. Vissink, L.U. Lahoda, J.L.N. Roodenburg, H. Reintsema, G.M. Raghoebar, M.J. Witjes, Accuracy of secondary maxillofacial reconstruction with prefabricated fibula grafts using 3D planning and guided reconstruction, Journal of Cranio-Maxillofacial Surgery 44 (2016) 392–399. https://doi.org/10.1016/j.jcms.2015.12.008.*
23. a, b *H. Hanken, C. Schablowsky, R. Smeets, M. Heiland, S. Sehner, B. Riecke, I. Nourwali, O. Vorwig, A. Gröbe, A. Al-Dam, Virtual planning of complex head and neck reconstruction results in satisfactory match between real outcomes and virtual models, Clin Oral Investig 19 (2015) 647–656. https://doi.org/10.1007/s00784-014-1291-5.*

24. ^S. Jeon, C.-O. Lee, Recent Approaches to Metal Artifact Reduction in X-Ray CT Imaging, in: Handbook of Mathematical Models and Algorithms in Computer Vision and Imaging, Springer International Publishing, Cham, 2023: pp. 347–377. https://doi.org/10.1007/978-3-030-98661-2_114.

25. ^M. Amirian, D. Barco, I. Herzig, F.-P. Schilling, Artifact Reduction in 3D and 4D Cone-Beam Computed Tomography Images With Deep Learning: A Review, IEEE Access 12 (2024) 10281–10295. https://doi.org/10.1109/ACCESS.2024.3353195.

26. ^M. Selles, J.A.C. van Osch, M. Maas, M.F. Boomsma, R.H.H. Wellenberg, Advances in metal artifact reduction in CT images: A review of traditional and novel metal artifact reduction techniques, Eur J Radiol 170 (2024) 111276. https://doi.org/10.1016/j.ejrad.2023.111276.

27. ^B.P. Kumar, V. Venkatesh, K.A.J. Kumar, B.Y. Yadav, S.R. Mohan, Mandibular Reconstruction: Overview, J Maxillofac Oral Surg 15 (2016) 425–441. https://doi.org/10.1007/s12663-015-0766-5.

28. ^K. Jagtiani, S. Gurav, G. Singh, K. Dholam, A review on the classification of mandibulectomy defects and suggested criteria for a universal description, J Prosthet Dent 132 (2024) 270–277. https://doi.org/10.1016/j.prosdent.2022.06.001.

29. ^R.C.W. Wong, H. Tideman, L. Kin, M.A.W. Merkx, Biomechanics of mandibular reconstruction: a review, Int J Oral Maxillofac Surg 39 (2010) 313–319. https://doi.org/10.1016/j.ijom.2009.11.003.

30. ^Y. Wang, G. Chen, N. Zhou, X. Huang, A new classification of mandible defects and condyle changed after mandible reconstruction with FFF, Heliyon 10 (2024) e25831. https://doi.org/10.1016/j.heliyon.2024.e25831.

31. ^S.-H. Lim, M.-K. Kim, S.-H. Kang, Precision of fibula positioning guide in mandibular reconstruction with a fibula graft, Head Face Med 12 (2016) 7. https://doi.org/10.1186/s13005-016-0104-2.

32. ^N. Casap, A. Wexler, R. Eliashar, Computerized Navigation for Surgery of the Lower Jaw: Comparison of 2 Navigation Systems, Journal of Oral and Maxillofacial Surgery 66 (2008) 1467–1475. https://doi.org/10.1016/j.joms.2006.06.272.

33. a, bR.H. Schepers, G.M. Raghoebar, A. Vissink, M.W. Stenekes, J. Kraeima, J.L. Roodenburg, H. Reintsema, M.J. Witjes, Accuracy of fibula reconstruction using patient-specific CAD/CAM reconstruction plates and dental implants: A new modality for functional reconstruction of mandibular defects, Journal of Cranio-Maxillofacial Surgery 43 (2015) 649–657. https://doi.org/10.1016/j.jcms.2015.03.015.

34. ^S.M. Roser, S. Ramachandra, H. Blair, W. Grist, G.W. Carlson, A.M. Christensen, K.A. Weimer, M.B. Steed, The Accuracy of Virtual Surgical Planning in Free Fibula Mandibular Reconstruction: Comparison of Planned and Final Results, Journal of Oral and Maxillofacial Surgery 68 (2010) 2824–2832. https://doi.org/10.1016/j.joms.2010.06.177.

35. ^*E. Zavattero, A. Bolzoni, G. Dell'Aversana, M. Santagata, O. Massarelli, A. Ferri, M. Della Monaca, C. Copelli, M. Gessaroli, S. Valsecchi, C. Borbon, G.A. Beltramini, G. Ramieri, V. Valentini, G.P. Tartaro, R. Cocchi, A. Varazzani, L. Califano, A. Baj, Accuracy of Fibula Reconstruction Using Patient-Specific Cad/Cam Plates: A Multicenter Study on 47 Patients, Laryngoscope 131 (2021). https://doi.org/10.1002/lary.29379.*
36. ^*M. Bevini, F. Vitali, F. Ceccariglia, G. Badiali, A. Tarsitano, Accuracy Evaluation of an Alternative Approach for a CAD-AM Mandibular Reconstruction with a Fibular Free Flap via a Novel Hybrid Roto-Translational and Surface Comparison Analysis, J Clin Med 12 (2023) 1938. https://doi.org/10.3390/jcm12051938.*

Declarations

Funding: Alberto Bedogni was supported by a research grant from Sintac s.r.l. (BEDO_COMM17_01: December 2017 - December 2019).

Potential competing interests: Giorgio Bedogni is co-founder and Chief Editor, and Alberto Bedogni is co-founder and Managing Editor, of Qeios, the platform on which this preprint is being posted.